Computer Modeling in Engineering & Sciences CMES, vol.122, no.1, pp.89-107, 2020

Adaptive Quasi Fixed-Time Orbit Control Around Asteroid with Performance Guarantees

Renyong Zhang[1], Caisheng Wei[2,*] and Zeyang Yin[3,*]

Abstract: This paper investigates a novel quasi fixed-time orbit tracking control method for spacecraft around an asteroid in the presence of uncertain dynamics and unknown uncertainties. To quantitatively characterize the transient and steady-state responses of orbit tracking error system, a continuous performance function is devised via using a quartic polynomial. Then, integrating backstepping control technique and barrier Lyapunov function leads to a quasi fixed-time convergent orbit tracking controller without using any fractional state information and symbolic functions. Finally, two groups of illustrative examples are employed to test the effectiveness of the proposed orbit control method.

Keywords: Prescribed performance, adaptive control, orbital control, asteroid.

1 Introduction

With the fast development of space explorations, small celestial bodies such as asteroids and comets have attracted wide attention. This is because that the asteroids have potential scientific significance and practical applications such as the mining of asteroid resources and navigation for interplanetary flight (e.g., [Jee, Khatib, Muellerschoen et al. (1988); Broschart and Scheeres (2005); Dai, Jing, Wang et al. (2018)] and references therein). In this sense, considerable research works on the small celestial bodies have sprung up in the existing literature. For example, Wie [Wie (2008)] investigated the dynamic modelling and control for the gravity tractor spacecraft used in the asteroid deflection. Kumar [Kumar (2008)] proposed a three-axis attitude control scheme for spacecraft rotating asteroids in an equatorial eccentric orbit. Vetrisano et al. [Vetrisano, Colombo and Vasile (2016)] presented a robust control law for the chaser spacecraft in the proximity motion to an asteroid with consideration of deflection acceleration and solar radiation pressure.

In order to obtain precise information about the surface characteristics, density, and

[1]Technology and Engineering Center for Space Utilization, Chinese Academy of Sciences, Beijing, 100094, China.
[2]School of Aeronautics and Astronautics, Central South University, Changsha, 410083, China.
[3]School of Astronautics, Northwestern Polytechnical University, Xi'an, 710072, China.
*Corresponding Authors: Caisheng Wei. Email: caisheng.wei@csu.edu.cn;
Zeyang Yin. Email: yinzy0126@foxmail.com.
Received: 17 July 2019; Accepted: 25 August 2019.

rotational rate, the chaser spacecraft is required to run around the target asteroid. Generally, the spacecraft is needed to track a closed orbit or hover over a fixed point around the asteroid [Ceriotti and Sanchez (2016); Guelman (2015)]. In this sense, efficient orbit and attitude control systems are pretty important. For example, a fuel-optimal control law for soft landing on an asteroid was developed by an improved homotopic approach by Yang et al. [Yang and Baoyin (2015)]. Zeng et al. [Zeng, Gong, Li et al. (2016)] analyzed the feasible hovering regions over spinning elongated asteroids. To enhance the robustness of the controller with respect to uncertainties and external disturbance, sliding mode control (SMC) technique has been widely utilized in the existing reported works such as adaptive control scheme for orbit tracking around asteroids by Lee et al. [Lee and Singh (2019)]. To accelerate the convergence rate, finite-time or fixed-time control via using improved SMC technique has attracted considerable attention (e.g., [Liu, Zhang, Sun et al. (2019); Yin, Luo and Wei (2019); Yang, Bai and Baoyin (2016)] and references therein). Wherein, finite-time hovering control laws around asteroids were devised by Lee et al. [Lee, Sanyal, Butcher et al. (2015); Yang, Bai and Baoyin (2016)] via using terminal SMC technique. Although the convergence time can be guaranteed, there are two inherent limitations required to tackle. The first one is the complex fractional state information used in the relevant controller design. This increases the computational load dramatically, which renders the corresponding control scheme ineffective in practice. The second one is the usage of symbolic function. This makes the relevant control scheme discontinuous, which is difficult to be implemented in practical systems. Thus, it deserves further investigations on the computationally simple orbit and attitude control methods with fast convergence rate.

Apart from the foregoing convergence rate, the rest transient and steady-state performance (like the undershoot, overshoot, tracking accuracy and etc) is also very important for orbit and attitude system. Thanks to Bechlioulis et al. [Bechlioulis and Rovithakis (2008)], an effective methodology, prescribed performance control (PPC), was proposed to quantitatively characterize the transient and steady-state performance of the controlled systems. Up till now, PPC has been widely used in many research fields including the flight control of hypersonic vehicle, constrained control of Euler-Lagrange systems, vibration suspension of half-car system, and image-based control of servo system [Wei, Luo, Dai et al. (2017b); Zhao, Song, Ma et al. (2017); Wei, Luo, Dai et al. (2017a); Hua, Chen, Li et al. (2018); Bechlioulis, Heshmati-alamdari, Karras et al. (2019)] and references therein). In the traditional PPC control schemes developed in aforementioned works, exponential performance function is used, which makes the relevant controlled tracking system exponentially convergent. To improve the convergence rate, combination of PPC and SMC technique was investigated by Li et al. [Li, Luo, Wang et al. (2018) and Liu, Liu and Jing (2018)]. Although effective, the inherent limitations of traditional finite-time or fixed-time control method cannot be avoided [Yin, Suleman, Luo et al. (2019); Yin, Luo and Wei (2019)]. Thus, more attention should be paid on the finite-time or fixed-time PPC without the foregoing twofold limitations.

Inspired by the above observations, this paper investigates a novel adaptive fixed-time PPC method for orbit tracking around asteroids. To the authors' best knowledge, it is the first

time to apply a fixed-time PPC scheme to solve the orbit tracking problem around asteroids. Compared with the existing works, the contributions of this work are twofold: 1) No fractional state information and symbolic functions are used in the relevant orbit tracking controller design, which renders the devised control scheme computationally simple and easily achievable in practice. 2) The fixed-time convergence and prescribed orbit tracking performance can be guaranteed a priori, which avoids tedious parameter regulations.

The remainder of this paper is organized as follows. The asteroid dynamics and problem formulation are stated in Section 2. Section 3 shows the quasi fixed-time orbit controller design. Two groups of illustrative examples are employed in Section 4. Some conclusions are drawn in Section 5.

1.1 Notations

T is the vector transpose. $|\bullet|$ denotes the absolute value of a real number. $\sigma(\bullet)$ is the eigenvalue of nonsingular matrix. $\mathbb{R}^n$ represents the set of n-dimensional real numbers.

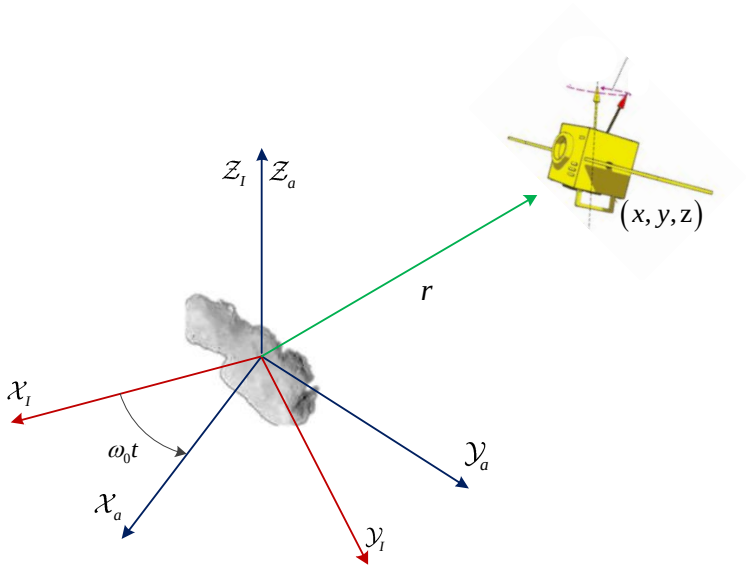

Figure 1: Coordinate system of the asteroid

2 Dynamics around asteroid and problem formulation

Before showing the asteroid dynamics, two important coordidate frames are defined. Namely, we use $(\mathcal{X}_a, \mathcal{Y}_a, \mathcal{Z}_a)$, $(\mathcal{X}_I, \mathcal{Y}_I, \mathcal{Z}_I)$ to, respectively, repesent the body-fixed axes and inertial coordidate frames of an asteroid with irregular shape (illustrated in Fig. 1). The origin of both the two frames is the center of mass of the asteroid. Without loss of generality, it is assumed that the asteroid only rotates along the axis $\mathcal{Z}_a$. The relative position between the asteroid and spacecraft is denoted by vector

$\boldsymbol{x}_{e1} = [x_{e1,1}, x_{e1,2}, x_{e1,3}]^T = [x, y, z]^T$. Then based on Lee and Singh's work [Lee and Singh (2019)], the approximate gravitational potential $\mathscr{P}(r)$ of the asteroid is obtained by

$$\mathscr{P}(r) = -\frac{Gm}{r} - \frac{G}{2r^3}\left(J_{11} + J_{22} + J_{33} - 3J_r\right), \tag{1}$$

with

$$J_r = \frac{1}{r^2}\boldsymbol{x}_{e1}^T \boldsymbol{J}_a \boldsymbol{x}_{e1}, \quad \boldsymbol{J}_a = \begin{bmatrix} J_{11} & J_{12} & J_{13} \\ J_{12} & J_{22} & J_{23} \\ J_{13} & J_{23} & J_{33} \end{bmatrix}, \quad r = \sqrt{x^2 + y^2 + z^2}, \tag{2}$$

where G is the universal gravitational constant, m represents the mass of the asteroid. $\boldsymbol{J}_a$ denotes the inertial matrix of the asteroid with J_{ij} $(i = 1, 2, 3, j = 1, 2, 3 \text{ and } i \leq j)$ being the elements. In general, m and $\boldsymbol{J}_a$ are unknown. r is the Euclidean norm of $\boldsymbol{x}_{e1}$. Accordingly, the corresponding gravitational acceleration is

$$\boldsymbol{f} = -\nabla\mathscr{P}(r) = -\begin{pmatrix} \frac{\partial\mathscr{P}(r)}{\partial x} \\ \frac{\partial\mathscr{P}(r)}{\partial y} \\ \frac{\partial\mathscr{P}(r)}{\partial z} \end{pmatrix}, \ \nabla\left(\frac{1}{r}\right) = -\frac{1}{r^2}\vec{\boldsymbol{i}}_r, \tag{3}$$

where $\vec{\boldsymbol{i}}_r = (1/r)\,\boldsymbol{x}_{e1}$ is the unit directional vector consisting of Cartesian vector components. Substituting (1) into (3) yields

$$\begin{aligned} \boldsymbol{f} = -\nabla\mathscr{P}(r) &= -\frac{Gm}{r^2}\vec{\boldsymbol{i}}_r - \frac{3G}{2r^4}\left(\sum_{i=1}^{3} J_{ii} - 5J_r\right)\vec{\boldsymbol{i}}_r - \frac{3G}{r^5}\boldsymbol{J}_a\boldsymbol{x}_{e1} \\ &= -\frac{3G}{2r^5}\begin{bmatrix} \left(J_{11}+J_{22}+J_{33}\right)x - \frac{5}{r^2}\left(J_{11}x^3 + J_{22}y^2x + J_{33}z^2x + 2J_{12}x^2y + 2J_{13}x^2z + 2J_{23}xyz\right) \\ \left(J_{11}+J_{22}+J_{33}\right)y - \frac{5}{r^2}\left(J_{11}x^2y + J_{22}y^3 + J_{33}z^2y + 2J_{12}xy^2 + 2J_{13}xyz + 2J_{23}y^2z\right) \\ \left(J_{11}+J_{22}+J_{33}\right)z - \frac{5}{r^2}\left(J_{11}x^2z + J_{22}y^2z + J_{33}z^3 + 2J_{12}xyz + 2J_{13}xz^2 + 2J_{23}yz^2\right) \end{bmatrix} \\ &\quad - \frac{Gm}{r^3}\boldsymbol{x}_{e1} - \frac{3G}{r^5}\boldsymbol{J}_a\boldsymbol{x}_{e1}. \end{aligned} \tag{4}$$

According to Lee et al. [Lee and Singh (2019)], for (4), a linearly parameterized form of the gravitational acceleration is obtained as

$$\boldsymbol{f} = \boldsymbol{\varphi}^T\boldsymbol{\theta}, \tag{5}$$

where $\boldsymbol{\theta} = [m, J_{11}, J_{22}, J_{33}, J_{12}, J_{13}, J_{23}]^T \in \mathbb{R}^7$, $\boldsymbol{\varphi} = [\boldsymbol{\varphi}_1, \boldsymbol{\varphi}_2, ..., \boldsymbol{\varphi}_7]^T \in \mathbb{R}^{7\times 3}$ with its detailed forms being expressed by

$$\boldsymbol{\varphi}_1 = -\frac{G}{r^3}\boldsymbol{x}_{e1}, \tag{6a}$$

$$\boldsymbol{\varphi}_2 = -\frac{3G}{2r^5}\left(1 - \frac{5x^2}{r^2}\right)\boldsymbol{x}_{e1} - \frac{3G}{r^5}[x, 0, 0]^T, \tag{6b}$$

$$\boldsymbol{\varphi}_3 = -\frac{3G}{2r^5}\left(1 - \frac{5y^2}{r^2}\right)\boldsymbol{x}_{e1} - \frac{3G}{r^5}[0, y, 0]^T, \tag{6c}$$

$$\boldsymbol{\varphi}_4 = -\frac{3G}{2r^5}\left(1 - \frac{5z^2}{r^2}\right)\boldsymbol{x}_{e1} - \frac{3G}{r^5}[0, 0, z]^T, \tag{6d}$$

$$\boldsymbol{\varphi}_5 = \frac{15G}{r^7}xy\boldsymbol{x}_{e1} - \frac{3G}{r^5}[y, x, 0]^T, \tag{6e}$$

$$\boldsymbol{\varphi}_6 = \frac{15G}{r^7}xz\boldsymbol{x}_{e1} - \frac{3G}{r^5}[z, 0, x]^T, \tag{6f}$$

$$\boldsymbol{\varphi}_7 = \frac{15G}{r^7}yz\boldsymbol{x}_{e1} - \frac{3G}{r^5}[0, z, y]^T. \tag{6g}$$

Remark 1. In practice, the mass and inertial parameters of the asteroid with an irregular shape are difficult to obtain. Thus, parameter vector $\boldsymbol{\theta}$ in (4) is known with uncertainties, which requires to estimate online. In the meanwhile, from (5), one can find that regressor function $\boldsymbol{\varphi}$ is with respect to the location parameters, which can be measured by the spacecraft directly. Thus, regressor function $\boldsymbol{\varphi}$ is known.

By defining $\boldsymbol{x}_{e2} = [x_{e2,1}, x_{e2,2}, x_{e2,3}]^T = \dot{\boldsymbol{x}}_{e1} = [\dot{x}, \dot{y}, \dot{z}]^T$, the relative motion equation is expressed by a strict-feedback form

$$\begin{cases} \dot{\boldsymbol{x}}_{e1} = \boldsymbol{x}_{e2} \\ \dot{\boldsymbol{x}}_{e2} = \boldsymbol{f} + \boldsymbol{g} + \boldsymbol{u} = \boldsymbol{\varphi}^T\boldsymbol{\theta} + \boldsymbol{g} + \boldsymbol{u} \end{cases}, \tag{7}$$

where $\boldsymbol{g} = \begin{bmatrix} 2\omega_0\dot{y} + \omega_0^2 x \\ -2\omega_0\dot{x} + \omega_0^2 y \\ 0 \end{bmatrix}$ is a known function with ω_0 being the rotational rate of the asteroid which can be observed by the spacecraft. $\boldsymbol{u} \in \mathbb{R}^3$ is the control input of the spacecraft to be determined later. Accordingly, the control objective of this paper is to devise an efficient controller to enable the spacecraft to track the desired orbit reference command with guaranteed transient and steady-state performance. Without loss of generality, the desired reference command is denoted by $\boldsymbol{x}_r = [x_r, y_r, z_r]^T \in \mathbb{R}^3$. To facilitate the following controller, a common assumption is imposed on the reference command $\boldsymbol{x}_r$, namely,

Assumption 1. Reference command $\boldsymbol{x}_r$ and its first-order derivative are known and bounded.

Remark 2. Assumption 1 is reasonable owing to the fact that the reference command can be designed by the users. Meanwhile, if the orbit reference command $\boldsymbol{x}_r$ is constant, then the spacecraft hovers over a fixed point of the asteroid. Otherwise, the spacecraft will move in a closed orbit around the asteroid.

3 Quasi fixed-time orbit control with performance guarantees

3.1 Prescribed performance for orbit tracking error system

Based on the foregoing dynamic model of asteroid, a quasi fixed-time orbit control method is investigated in this part. Before moving, a vital definition is given as follows.

Definition 1. (Quasi fixed-time control) For the relative motion in (6), quasi fixed-time orbit tracking control can be achieved if and only if the orbit tracking error satisfies $\lim_{t\geq t_f} \|\boldsymbol{x}_{e1}(t) - \boldsymbol{x}_r(t)\| \leq e_v$ for any setting time t_f (e_v is a non-negative constant).

Remark 3. In *Definition 1*, according to Liu et al. [Liu, Zhang, Sun et al. (2019); Yin, Luo and Wei (2019)], when $e_v = 0$, then the orbit tracking error system will be fixed-time convergent. In general, 'quasi fixed-time or fixed-time convergent' can be also called as 'finite-time convergent'. However, In practical space missions, when expected tracking accuracy is achieved, the mission requirement can be met in the presence of uncertain dynamics and space perturbations. Thus, quasi fixed-time control is practically useful.

To proceed, define the orbit tracking error $\boldsymbol{\varepsilon} = [\varepsilon_1, \varepsilon_2, \varepsilon_3]^T = \boldsymbol{x}_{e1} - \boldsymbol{x}_r$. Then, in order to guarantee the transient and steady-state performance of the orbit tracking system, the following performance constraint is imposed

$$-\rho_i(t) < \varepsilon_i < \rho_i(t) \quad (i = 1, 2, 3), \tag{8}$$

where $\rho_i(t)$ is the performance function to be determined later. Different from the traditional exponentially convergent performance function, inspired by Zhang et al. [Zhang and Duan (2014); Liu, Shao and Ma (2019)], in this paper, a fixed-time convergent performance function is devised. Its detailed form is given by

$$\rho_i(t) = \begin{cases} \rho_{i,0} + \sum_{j=1}^{4} \varrho_{i,j} t^j, & t \leq t_{i,f} \\ \rho_{i,\infty}, & t > t_{i,f} \end{cases}, \quad \dot{\rho}_i(t) = \begin{cases} \sum_{j=1}^{4} j\varrho_{i,j} t^{j-1}, & t \leq t_{i,f} \\ 0, & t > t_{i,f} \end{cases}, \tag{9}$$

where $\rho_{i,0} > \rho_{i,\infty} > 0$ $(i = 1, 2, 3)$ are positive design constants. $t_{i,f}$ is the upper bound of convergent time. $\varrho_{i,j}$ $(j = 1, 2, 3, 4)$ are constants, which are determined later. To guarantee the fixed-time convergence of the performance function, namely, $\forall t \geq t_{i,f}$, $\rho_i(t) = \rho_{i,\infty}$, parameters $\varrho_{i,j}$ $(j = 1, 2, 3, 4)$ satisfy

$$\begin{cases} \rho_i(0) = \rho_{i,0} > 0 \\ \dot{\rho}_i(0) = \varrho_{i,1} = 0 \\ \rho_i(t_{i,f}) = \rho_{i,0} + \varrho_{i,1} t_{i,f} + \varrho_{i,2} t_{i,f}^2 + \varrho_{i,3} t_{i,f}^3 + \varrho_{i,4} t_{i,f}^4 = \rho_{i,\infty} \\ \dot{\rho}_i(t_{i,f}) = \varrho_{i,1} + 2\varrho_{i,2} t_{i,f} + 3\varrho_{i,3} t_{i,f}^2 + 4\varrho_{i,4} t_{i,f}^3 = 0 \\ \ddot{\rho}_i(t_{i,f}) = 2\varrho_{i,2} + 6\varrho_{i,3} t_{i,f} + 12\varrho_{i,4} t_{i,f}^2 = 0 \end{cases}. \tag{10}$$

By solving the above Eq. (10), parameters $\varrho_{i,j}$ $(j = 1, 2, 3, 4)$ can be obtained. Accordingly, performance function $\rho(t)$ in (9) can be calculated.

Remark 4. When the parameter $\rho_{i,\infty}$ in (9) is set as a sufficiently small value, then one can find that the orbit tracking error system can be steered to zero around the time

instant t_f. However, high tracking accuracy requires sufficiently large control input. In this case, actuator saturation is easily caused. To deal with this problem, there exist two potential methods. The first one is the trial-and-error method. Via using this method, the value distribution of parameter $\rho_{i,\infty}$ can be obtained with some offline tests when actuator saturation does not occur. The second one is constructing an auxiliary system to remove the negative effect of the saturation constraint. Readers of interest can refer to Esfandiari et al. [Esfandiari, Abdollahi and Talebi (2014); Luo, Wei, Dai et al. (2018)], which is omitted for brevity. Thus, in practice, $\rho_{i,\infty}$ can be chosen based on the task requirement (like the orbit tracking accuracy) and actuator saturation. According to *Definition 1*, the relevant orbit tracking error system is quasi fixed-time convergent.

Remark 5. There are three key parameters, i.e., $\rho_{i,0},\ \rho_{i,\infty},\ t_f$ involved in $\rho_i(t)$. In general, parameter $\rho_{i,0}$ should satisfy $\rho_{i,0} > |\varepsilon_i(0)|$ based on (8). Parameter $\rho_{i,\infty}$ is relevant to the orbit tracking accuracy, which can be chosen as *Remark 4* presents. $t_{i,f}$ denotes the convergence time, which can be chosen based on the practical engineering requirement.

3.2 Quasi fixed-time controller design

To facilitate the subsequent controller design, backstepping technique is used to construct the relevant orbit tracking controller. In the backstepping technique, two steps are involved in the controller design.

Step 1. Before moving, define the standard orbit tracking error $\eta_{1,i} = \frac{\varepsilon_i}{\rho_i(t)} \in (-1,1)$. Then, to guarantee the prescribed performance in (8), the first Lyapunov function is constructed as

$$V_1 = \frac{1}{2}\sum_{j=1}^{3}\frac{\eta_{1,j}^2}{1-\eta_{1,j}^2}. \tag{11}$$

Taking time derivative of V_1 gets

$$\begin{aligned}\dot{V}_1 &= \frac{1}{2}\sum_{j=1}^{3}\frac{2\eta_{1,j}\dot{\eta}_{1,j}\left(1-\eta_{1,j}^2\right)+2\eta_{1,j}^3\dot{\eta}_{1,j}}{\left(1-\eta_{1,j}^2\right)^2}\\ &= \sum_{j=1}^{3}\frac{\eta_{1,j}}{\left(1-\eta_{1,j}^2\right)^2}\dot{\eta}_{1,j} = \sum_{j=1}^{3}\frac{\eta_{1,j}}{\left(1-\eta_{1,j}^2\right)^2}\left(\frac{\dot{\varepsilon}_i\rho_j(t)-\varepsilon_i\dot{\rho}_j(t)}{\rho_j^2(t)}\right)\\ &= \sum_{j=1}^{3}\frac{\eta_{1,j}}{\left(1-\eta_{1,j}^2\right)^2\rho_j(t)}\left(\dot{x}_{e1,j}-\dot{x}_{r,j}-\frac{\varepsilon_j\dot{\rho}_j(t)}{\rho_j(t)}\right)\end{aligned} \tag{12}$$

Define the coordinate transformation $\eta_{2,j} = x_{e2,j} - \gamma_j\ (j=1,2,3)$ with γ_j being the output of the following filter

$$\tau_j^*\dot{\gamma}_j + \gamma_j = \alpha_j\quad(\gamma_j(0) = \alpha_j(0)), \tag{13}$$

where $\tau_j^* = \frac{\tau_j}{1+\tau_j\hat{\omega}_j}$ with $\hat{\omega}_j$ being the estimation value for unknown parameter ω_j, which is given later. α_j is the following designed virtual controller. $\tau_j \in (0,4)$ is a positive

constant. The filter error in (13) is defined as $\delta_j = \gamma_j - \alpha_j$. Substituting $\eta_{2,j} = x_{e2,j} - \gamma_j$ and $\delta_j = \gamma_j - \alpha_j$ into (11) yields

$$\begin{aligned}\dot{V}_1 &= \sum_{j=1}^{3} \frac{\eta_{1,j}}{\left(1-\eta_{1,j}^2\right)^2 \rho_j(t)} \left(\dot{x}_{e1,j} - \dot{x}_{r,j} - \frac{\varepsilon_i \dot{\rho}_i(t)}{\rho_i(t)}\right) \\ &= \sum_{j=1}^{3} \frac{\eta_{1,j}}{\left(1-\eta_{1,j}^2\right)^2 \rho_j(t)} \left(\gamma_j + \eta_{2,j} - \dot{x}_{r,j} - \frac{\varepsilon_i \dot{\rho}_i(t)}{\rho_i(t)}\right) \\ &= \sum_{j=1}^{3} \frac{\eta_{1,j}}{\left(1-\eta_{1,j}^2\right)^2 \rho_j(t)} \left(\alpha_j + \eta_{2,j} + \delta_j - \dot{x}_{r,j} - \frac{\varepsilon_i \dot{\rho}_i(t)}{\rho_i(t)}\right)\end{aligned} \quad . \tag{14}$$

Based on (14), the following inequality holds

$$\frac{\eta_{1,j}}{\left(1-\eta_{1,j}^2\right)^2 \rho_i(t)} (\eta_{2,j} + \delta_j) \leq \frac{2\eta_{1,j}^2}{\left(1-\eta_{1,j}^2\right)^4 \rho_j^2(t)} + \frac{1}{4}\left(\eta_{2,j}^2 + \delta_j^2\right). \tag{15}$$

Accordingly, the virtual controller α_j $(j = 1, 2, 3)$ is devised as

$$\alpha_j = -k_{1,j}\eta_{1,j} + \dot{x}_{r,j} + \frac{\varepsilon_i \dot{\rho}_i(t)}{\rho_i(t)} - \frac{2\eta_{1,j}}{\left(1-\eta_{1,j}^2\right)^2 \rho_j(t)}, \tag{16}$$

where $k_{1,j}$ is a positive control gain. According to Young's inequality in Dragomir [Dragomir (2017)], substituting (16) into (14) yields

$$\dot{V}_1 \leq -\sum_{j=1}^{3} \frac{k_{1,j}\eta_{1,j}^2}{\left(1-\eta_{1,j}^2\right)^2 \rho_j(t)} + \frac{1}{4}\sum_{j=1}^{3}\left(\eta_{2,j}^2 + \delta_j^2\right). \tag{17}$$

Step 2. In this step, we define the following Lyapunov function

$$V_2 = V_1 + \frac{1}{2}\boldsymbol{\eta}_2^T\boldsymbol{\eta}_2 + \frac{1}{2}\tilde{\boldsymbol{\theta}}^T\boldsymbol{\Gamma}^{-1}\tilde{\boldsymbol{\theta}}, \tag{18}$$

where $\tilde{\boldsymbol{\theta}} = \boldsymbol{\theta} - \hat{\boldsymbol{\theta}}$ denotes the estimation error. Owing to the fact that $\boldsymbol{\theta}$ is constant, then $\dot{\tilde{\boldsymbol{\theta}}} = -\dot{\hat{\boldsymbol{\theta}}}$. $\boldsymbol{\eta}_2 = [\eta_{2,1}, \eta_{2,2}, \eta_{2,3}]^T \in \mathbb{R}^3$. $\boldsymbol{\Gamma} \in \mathbb{R}^{7\times 7}$ is a positive-definite diagonal matrix. With consideration of $\dot{\eta}_{2,j} = \dot{x}_{e2,j} - \dot{\gamma}_i$ and (7), the time-derivative of V_2 is

$$\begin{aligned}\dot{V}_2 &= \dot{V}_1 + \boldsymbol{\eta}_2^T\dot{\boldsymbol{\eta}}_2 + \tilde{\boldsymbol{\theta}}^T\boldsymbol{\Gamma}^{-1}\dot{\tilde{\boldsymbol{\theta}}} \\ &= \dot{V}_1 + \boldsymbol{\eta}_2^T(\dot{\boldsymbol{x}}_{e2} - \dot{\boldsymbol{\gamma}}) + \tilde{\boldsymbol{\theta}}^T\boldsymbol{\Gamma}^{-1}\dot{\tilde{\boldsymbol{\theta}}} \\ &= \dot{V}_1 + \boldsymbol{\eta}_2^T(\boldsymbol{f} + \boldsymbol{g} + \boldsymbol{u} - \dot{\boldsymbol{\gamma}}) + \tilde{\boldsymbol{\theta}}^T\boldsymbol{\Gamma}^{-1}\dot{\tilde{\boldsymbol{\theta}}} \\ &= \dot{V}_1 + \boldsymbol{\eta}_2^T\left(\boldsymbol{\varphi}^T\boldsymbol{\theta} + \boldsymbol{g} + \boldsymbol{u} - \dot{\boldsymbol{\gamma}}\right) + \tilde{\boldsymbol{\theta}}^T\boldsymbol{\Gamma}^{-1}\dot{\tilde{\boldsymbol{\theta}}} \\ &\leq -\sum_{j=1}^{3} \frac{k_{1,j}\eta_{1,j}^2}{\left(1-\eta_{1,j}^2\right)^2 \rho_j(t)} + \frac{1}{4}\sum_{j=1}^{3}\left(\eta_{2,j}^2 + \delta_j^2\right) + \boldsymbol{\eta}_2^T\left(\boldsymbol{\varphi}^T\boldsymbol{\theta} + \boldsymbol{g} + \boldsymbol{u} - \dot{\boldsymbol{\gamma}}\right) - \tilde{\boldsymbol{\theta}}^T\boldsymbol{\Gamma}^{-1}\dot{\hat{\boldsymbol{\theta}}}.\end{aligned}$$

(19)

where $\boldsymbol{\gamma} = [\gamma_1, \gamma_2, \gamma_3]^T$. Accordingly, the relevant actual control input is devised as

$$\boldsymbol{u} = -\boldsymbol{k}_2\boldsymbol{\eta}_2 - \frac{1}{4}\boldsymbol{\eta}_2 + \dot{\boldsymbol{\gamma}} - \boldsymbol{\varphi}^T\hat{\boldsymbol{\theta}} - \boldsymbol{g}, \tag{20}$$

where $\boldsymbol{k}_2 \in \mathbb{R}^{3\times 3}$ is the control gain matrix, which is positive-definite. The corresponding adaptive scheme for unknown parameter $\boldsymbol{\theta}$ is developed as

$$\dot{\hat{\boldsymbol{\theta}}} = \boldsymbol{\Gamma}\boldsymbol{\varphi}\boldsymbol{\eta}_2 \tag{21}$$

Substituting (20) and (21) into (19) yields

$$\begin{aligned}
\dot{V}_2 &\leq -\sum_{j=1}^{3}\frac{k_{1,j}\eta_{1,j}^2}{\left(1-\eta_{1,j}^2\right)^2\rho_j(t)} - \sigma_{\min}(\boldsymbol{k}_2)\eta_2^T\eta_2 + \frac{1}{4}\sum_{j=1}^{3}\delta_j^2 + \boldsymbol{\eta}_2^T\boldsymbol{\varphi}^T\left(\boldsymbol{\theta}-\hat{\boldsymbol{\theta}}\right) - \tilde{\boldsymbol{\theta}}^T\boldsymbol{\Gamma}^{-1}\dot{\hat{\boldsymbol{\theta}}} \\
&= -\sum_{j=1}^{3}\frac{k_{1,j}\eta_{1,j}^2}{\left(1-\eta_{1,j}^2\right)^2\rho_j(t)} - \sigma_{\min}(\boldsymbol{k}_2)\boldsymbol{\eta}_2^T\boldsymbol{\eta}_2 + \frac{1}{4}\sum_{j=1}^{3}\delta_j^2 + \boldsymbol{\eta}_2^T\boldsymbol{\varphi}^T\tilde{\boldsymbol{\theta}} - \tilde{\boldsymbol{\theta}}^T\boldsymbol{\Gamma}^{-1}\dot{\hat{\boldsymbol{\theta}}} \\
&= -\sum_{j=1}^{3}\frac{k_{1,j}\eta_{1,j}^2}{\left(1-\eta_{1,j}^2\right)^2\rho_j(t)} - \sigma_{\min}(\boldsymbol{k}_2)\boldsymbol{\eta}_2^T\boldsymbol{\eta}_2 + \frac{1}{4}\sum_{j=1}^{3}\delta_j^2 + (\boldsymbol{\varphi}\boldsymbol{\eta}_2)^T\tilde{\boldsymbol{\theta}} - \tilde{\boldsymbol{\theta}}^T\boldsymbol{\Gamma}^{-1}\dot{\hat{\boldsymbol{\theta}}} \\
&= -\sum_{j=1}^{3}\frac{k_{1,j}\eta_{1,j}^2}{\left(1-\eta_{1,j}^2\right)^2\rho_j(t)} - \sigma_{\min}(\boldsymbol{k}_2)\boldsymbol{\eta}_2^T\boldsymbol{\eta}_2 + \frac{1}{4}\sum_{j=1}^{3}\delta_j^2.
\end{aligned} \tag{22}$$

Based on the foregoing controller design in two steps, one crucial result can be concluded in the following theorem.

Theorem 1. The desired orbit reference command can be tracked with guaranteed prescribed performance under the devised controller and adaptive scheme. Meanwhile, all the involved closed-loop signals are uniformly ultimately bounded by devising the following adaptive scheme for the first-order filter:

$$\dot{\hat{\omega}}_j = -\beta_{1,j}\hat{\omega}_j + \delta_j^2 \quad (j = 1, 2, 3). \tag{23}$$

where $\beta_{1,j}$ represents a positive constant.

Proof. To prove Theorem 1, the following Lyapunov function is defined

$$V_3 = V_2 + \frac{1}{2}\boldsymbol{\delta}^T\boldsymbol{\delta} + \frac{1}{2}\tilde{\boldsymbol{\omega}}^T\tilde{\boldsymbol{\omega}}, \tag{24}$$

where $\boldsymbol{\delta} = [\delta_1, \delta_2, \delta_3]^T$ is the filter estimation error. $\tilde{\boldsymbol{\omega}} = \boldsymbol{\omega} - \hat{\boldsymbol{\omega}}$ denotes the estimation error for unknown parameter $\boldsymbol{\omega}$ with its detailed meaning being given later. Then, based on

the first-order filter (13), the time-derivative of V_3 is equal to

$$\begin{aligned}\dot{V}_3 &= \dot{V}_2 + \boldsymbol{\delta}^T\dot{\boldsymbol{\delta}} + \tilde{\boldsymbol{\omega}}^T\dot{\tilde{\boldsymbol{\omega}}} \\ &= \dot{V}_2 + \sum_{j=1}^{3}\delta_j\left(\dot{\gamma}_j - \dot{\alpha}_j\right) + \tilde{\boldsymbol{\omega}}^T\dot{\tilde{\boldsymbol{\omega}}} \\ &= \dot{V}_2 + \sum_{j=1}^{3}\delta_i\left(\frac{1+\tau_j\hat{\omega}_j}{\tau_j}\left(-\gamma_j+\alpha_j\right) - \dot{\alpha}_j\right) + \sum_{j=1}^{3}\tilde{\omega}_j\dot{\tilde{\omega}}_j \\ &= \dot{V}_2 - \sum_{j=1}^{3}\left(\frac{1}{\tau_j} + \hat{\omega}_j\right)\delta_j^2 - \sum_{j=1}^{3}\left(\delta_j\dot{\alpha}_j\right) + \sum_{j=1}^{3}\tilde{\omega}_j\dot{\tilde{\omega}}_j.\end{aligned} \tag{25}$$

Based on (13) and (22), by applying Young's inequality based on Dragomir (2017), (25) becomes

$$\begin{aligned}\dot{V}_3 \le &-\sum_{j=1}^{3}\frac{k_{1,j}\eta_{1,j}^2}{\left(1-\eta_{1,j}^2\right)^2\rho_j\left(t\right)} - \sigma_{\min}(\boldsymbol{k}_2)\boldsymbol{\eta}_2^T\boldsymbol{\eta}_2 - \sum_{j=1}^{3}\left(\frac{1}{\tau_j} - \frac{1}{4} + \hat{\omega}_j\right)\delta_j^2 \\ &+ \sum_{j=1}^{3}\left|\dot{\alpha}_j\right|^2\delta_j^2 + \sum_{j=1}^{3}\tilde{\omega}_j\dot{\tilde{\omega}}_j + \frac{3}{4}.\end{aligned} \tag{26}$$

Considering that the virtual controller α_j is continuous with respect to controlled states, thus, its time-derivative is bounded. Namely, without loss of generality, it is assumed that $|\dot{\alpha}_j|$ satisfies $0 \le |\dot{\alpha}_j|^2 \le \omega_j$ with ω_j being an unknown constant. Consequently, (26) becomes

$$\begin{aligned}\dot{V}_3 \le &-\sum_{j=1}^{3}\frac{k_{1,j}\eta_{1,j}^2}{\left(1-\eta_{1,j}^2\right)^2\rho_j\left(t\right)} - \sigma_{\min}(\boldsymbol{k}_2)\boldsymbol{\eta}_2^T\boldsymbol{\eta}_2 - \sum_{j=1}^{3}\left(\frac{1}{\tau_j} - \frac{1}{4}\right)\delta_j^2 \\ &+ \sum_{j=1}^{3}\left(\omega_j - \hat{\omega}_j\right)\delta_j^2 + \sum_{j=1}^{3}\tilde{\omega}_j\dot{\tilde{\omega}}_j + \frac{3}{4} \\ \le &-\sum_{j=1}^{3}\frac{k_{1,j}\eta_{1,j}^2}{\left(1-\eta_{1,j}^2\right)^2\rho_j\left(t\right)} - \sigma_{\min}(\boldsymbol{k}_2)\boldsymbol{\eta}_2^T\boldsymbol{\eta}_2 - \sum_{j=1}^{3}\left(\frac{1}{\tau_j} - \frac{1}{4}\right)\delta_j^2 + \sum_{j=1}^{3}\tilde{\omega}_j\left(\delta_j^2 - \dot{\hat{\omega}}_j\right) + \frac{3}{4} \\ \le &-\sum_{j=1}^{3}\frac{k_{1,j}\eta_{1,j}^2}{\left(1-\eta_{1,j}^2\right)^2\rho_j\left(t\right)} - \sigma_{\min}(\boldsymbol{k}_2)\boldsymbol{\eta}_2^T\boldsymbol{\eta}_2 - \sum_{j=1}^{3}\left(\frac{1}{\tau_j} - \frac{1}{4}\right)\delta_j^2 - \frac{1}{2}\sum_{j=1}^{3}\beta_{1,j}\hat{\omega}_j^2 + \kappa_0,\end{aligned} \tag{27}$$

where $\kappa_0 = \frac{3}{4} + \frac{1}{2}\sum_{j=1}^{3}\beta_{1,j}\omega_j^2$ is an unknown constant. Due to $\tau_j \in (0,4)$, the controlled orbit tracking error system is uniformly ultimately bounded. In this sense, the prescribed performance for orbit tracking error system in (8) can be guaranteed in the whole time domain. This completes the proof of Theorem 1. ■

Remark 6. As shown in Theorem 1, one can find that a quasi fixed-time convergent orbit tracking error system can be guaranteed with the developed controller and adaptive schemes in (20), (21) and (23). Compared with the existing works on fixed-time control, one can

Table 1: Parameters of 433 Eros asteroid

Parameter	Value	Unit
m	6.6871×10^{15}	kg
J_{11}	1.117×10^{17}	kg.km^2
J_{22}	4.793×10^{17}	kg.km^2
J_{33}	4.987×10^{17}	kg.km^2
J_{12}	6.232×10^{16}	kg.km^2
J_{13}	-2.257×10^{14}	kg.km^2
J_{23}	-2.589×10^{13}	kg.km^2
ω_0	3.312×10^{-4}	rad/s

find that the developed control scheme is very computationally simple due to the fact that no fractional state feedback information and symbolic function are used. Meanwhile, the transient and steady-state performance of the orbit tracking error system can be guaranteed a priori, which is pretty advantageous in practice. However, this does not means that the required control efforts are less than the existing works. It is easy to find that excellent transient and steady-state performance requires large control input. So in practice, the controllability and fuel assumptions should be taken into account to choose the parameters involved in the performance function.

Remark 7. Based on Theorem 1, one can find that only quasi fixed-time convergence can be guaranteed under the devised control scheme. To further improve the orbit tracking accuracy (like achieving fixed-time stability), SMC technique, as a potential way, can be applied to construct the relevant controller. However, the inherent drawbacks brought by SMC technique cannot be avoided as *Remark 5* discussed.

Remark 8. In this work, the symmetric performance constraint in (8) is considered. To adjust the overshoot or undershoot of the controlled system, asymmetric performance constraint has been considered in some works like in Bechlioulis et al. [Bechlioulis and Rovithakis (2008); Wei, Luo, Dai et al. (2017a)]. In this case, the barrier Lyapunov function in (11) can be chosen as $V_1 = \frac{1}{2}\left[\hbar\left(\eta_{1,i}\left(t\right)\right)\log\frac{k_b^2}{k_b^2-\eta_{1,i}^2} + \left(1-\hbar\left(\eta_{1,i}\left(t\right)\right)\right)\log\frac{k_a^2}{k_a^2-\eta_{1,i}^2}\right]$ with $k_a,\ k_b \in (0,1)$ being the relevant constant parameters according to Liu et al. [Liu, Lu, Li et al. (2016)]. $\hbar\left(z\left(t\right)\right) \in \{0,1\}$ is chosen based on the standard error $\eta_{1,i}$. The rest steps presented in Subsection 3.1 are the same.

4 Illustrative simulations

To validate the effectiveness of the proposed control method, two groups of illustrative examples are organized in this section. Wherein, the model of 433 Eros is chosen as the simulation object. According to Scheeres et al. [Scheeres, Williams and Miller (2000); Lee and Singh (2019)], the detailed parameters of 433 Eros asteroid are presented in Tab. 1.

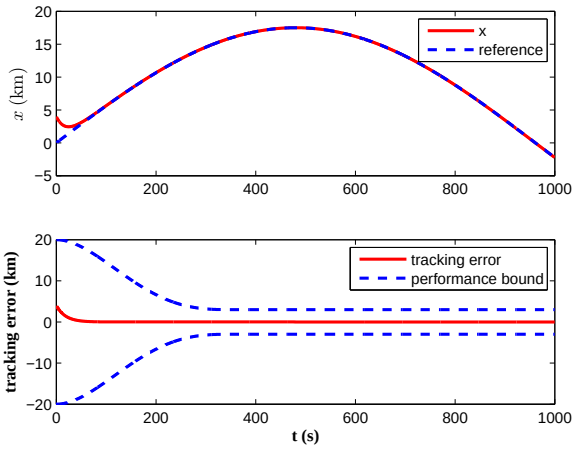

Figure 2: Trajectory of position x in orbit tracking

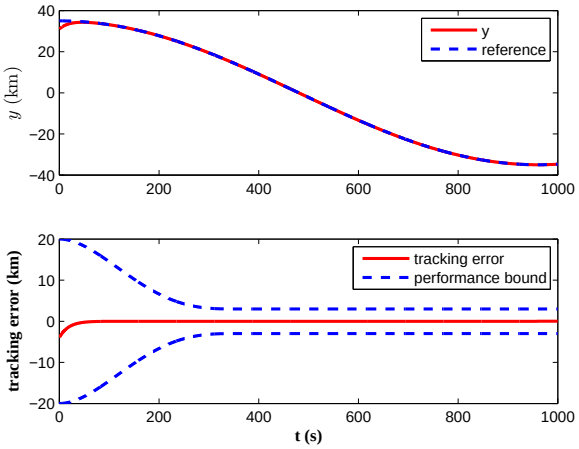

Figure 3: Trajectory of position y in orbit tracking

4.1 Tracking control in a closed orbit around the asteroid

In practical orbit mission, the spacecraft is often required to track a closed orbit around the asteroid in order to obtain precise information about the surface characteristics and size of the asteroid. Thus, in this part, based on the asteroid parameters in Tab. 1, simulation scenario about tracking a closed orbit is organized. Without loss of generality, the desired reference trajectory is generated by the following equations

$$x_r = 0.5R\sin(\omega_e t)\,,\ y_r = R\cos(\omega_e t)\,,\ z_r = R\sin(\omega_e t)\,, \tag{28}$$

where $R = 35$ km, $\omega_e = 9.87\omega_0$. The initial unknown parameter $\hat{\boldsymbol{\theta}}$ is set as 80% of the nominal values shown in Tab. 1. The corresponding simulation results are demonstrated in Figs. 2-8.

Table 2: Simulation parameters in orbit tracking control

Equation	Parameters
Eq. (9)	$\rho_{i,0} = 20, \rho_{i,\infty} = 2,\ t_{i,f} = 350\ (i = 1, 2, 3)$
Eq. (13)	$\tau_1 = 0.1, \tau_2 = 0.1, \tau_3 = 0.2$
Eq. (16)	$k_{1,1} = k_{1,2} = k_{1,3} = 1$
Eq. (18)	$\mathbf{\Gamma} = \mathrm{diag}\{10^4, 10^8, 10^8, 10^8, 10^6, 10^2, 1\} \times 10^{27}$
Eq. (20)	$\boldsymbol{k}_2 = \mathrm{diag}\{3, 3, 3\}$
Eq. (23)	$\beta_{1,1} = \beta_{1,2} = \beta_{1,3} = 0.1$

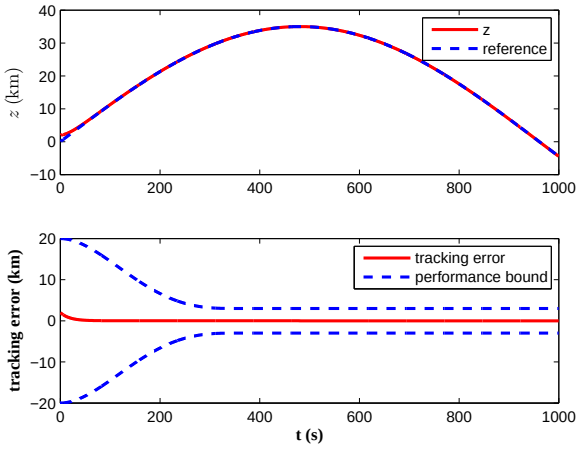

Figure 4: Trajectory of position z in orbit tracking

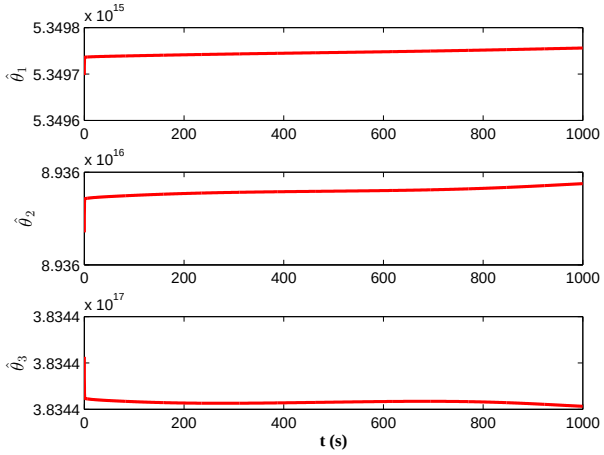

Figure 5: Time responses of adaptive parameters $\hat{\theta}_j\ (j = 1, 2, 3)$

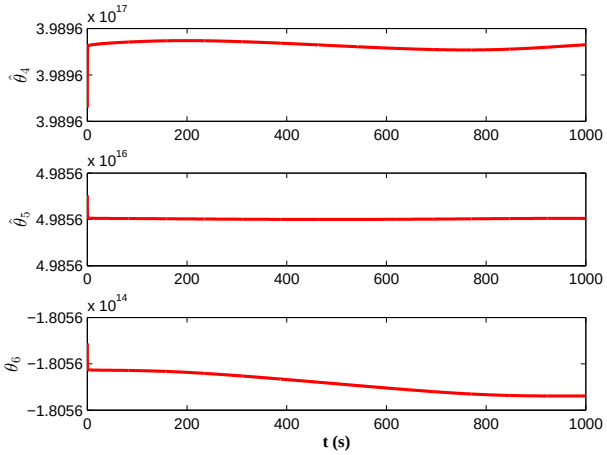

Figure 6: Time responses of adaptive parameters $\hat{\theta}_j$ $(j = 4, 5, 6)$

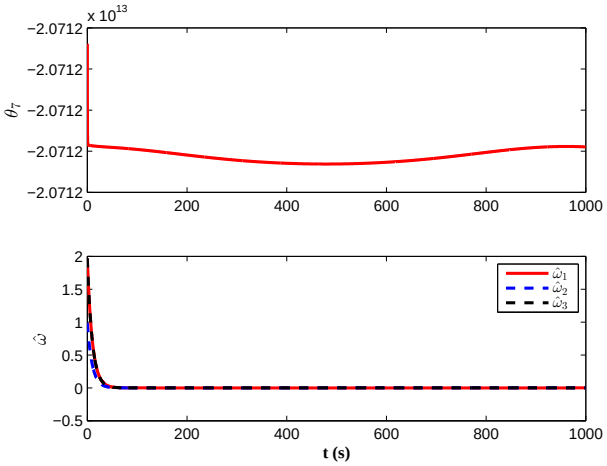

Figure 7: Time responses of adaptive parameters $\hat{\theta}_7$ and $\hat{\omega}_j$ $(j = 1, 2, 3)$

As presented in Figs. 2-8, one can conclude that: 1) The desired orbit reference trajectory can be tracked within 350 s. And the preassigned transient and steady-state performance of orbit tracking error system is guaranteed in the whole time domain (shown in Figs. 2-4). 2) Figs. 5-7 show that the estimation procedure for unknown parameters are convergent, which implies the effectiveness of the proposed adaptive schemes. 3) Fig. 8 presents that the control input of the spacecraft is continuous with respect to time. To be brief, the simulation results demonstrate that the proposed control method can solve the orbit tracking problem effectively.

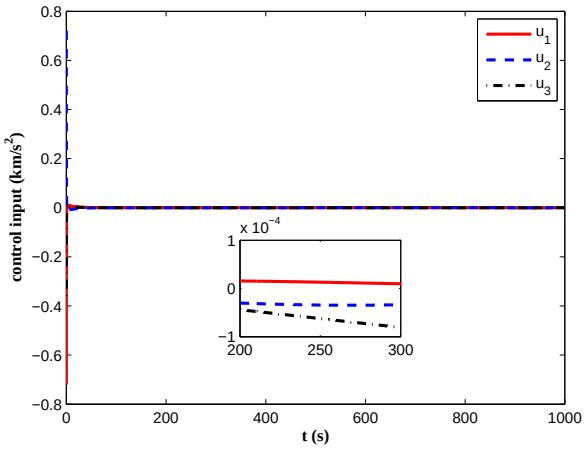

Figure 8: Control input of the spacecraft in orbit tracking

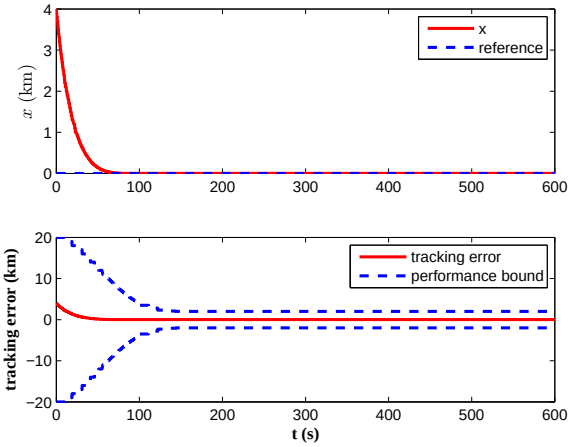

Figure 9: Trajectory of position x in hovering control

4.2 Hovering control over a fixed point of the asteroid

To further validate the proposed control method, in this part, hovering control over a fixed-time of the asteroid is organized. Without loss of generality, the desired fixed point is chosen as $\boldsymbol{x}_r = [0, 0, 8]^T$ km. The expected convergent time $t_{i,f}$ $(i = 1, 2, 3)$ is set as 150 s in this simulation scenario. The rest simulation parameters are the same as those in Tab. 2. Moreover, the initial simulation conditions are the same as those in the first simulation example. To test the robustness of the proposed control method, it is assumed that there are 30% random uncertainty in the nominal value of the inertial parameters of the asteroid. Then, the relevant simulation results are shown in Figs. 9-12.

As illustrated in Figs. 9-12, one can conclude that: 1) The spacecraft can hover over the

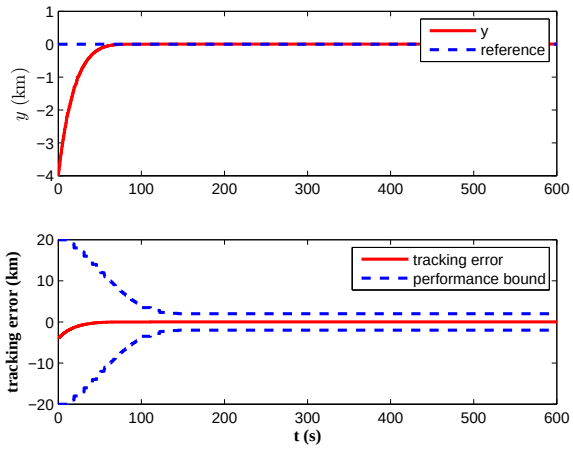

Figure 10: Trajectory of position y in hovering control

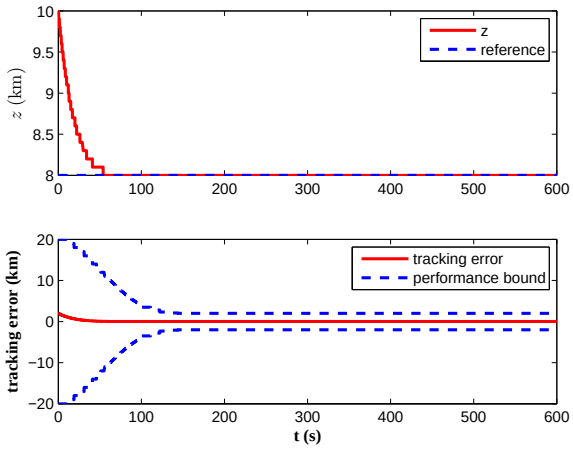

Figure 11: Trajectory of position z in hovering control

desired fixed point around the asteroid stably with the convergence time being less than 150 s. Meanwhile, the prescribed transient and steady-state performance of orbit tracking error system is achieved within the expected convergent time (shown in Figs. 9-11). 2) The proposed control method is robust with respect to unexpected dynamic uncertainty and the relevant control input is quite stable (depicted in Fig. 12).

To sum up, the foregoing two simulation scenarios demonstrate the effectiveness and robustness of the proposed control method in orbit tracking around asteroid in the presence of unknown dynamics and uncertainties.

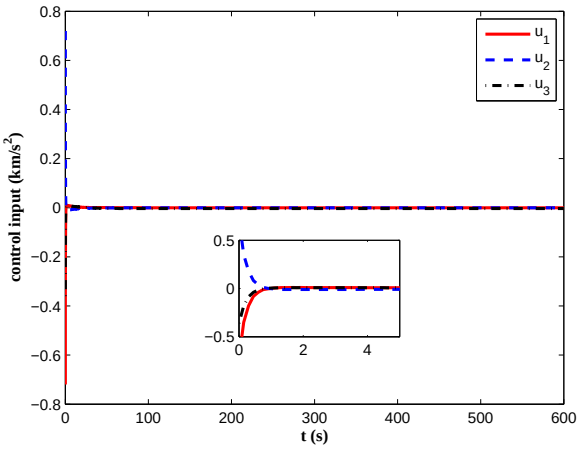

Figure 12: Control input of the spacecraft in hovering control

5 Conclusion

An adaptive quasi fixed-time orbit tracking control method has been developed in this paper. First, a fixed-time convergence performance function is designed with which the performance constraint is imposed on the orbit tracking error system. Then, a barrier Lyapunov function is constructed to remove the performance constraint. For the cascaded orbit tracking system, backstepping technique is applied to develop the relevant adaptive controller. Different from the existing works on finite-time or fixed-time control, the prominent advantage of the proposed control method is that no fractional state feedback information and symbolic functions are used in the relevant orbit controller design. While the fixed-time convergence is achieved with performance guarantees. The two groups of illustrative simulation examples show that the expected orbit reference trajectory can be tracked within the desired time. Meanwhile, the proposed orbit control method is robust with respect to unknown dynamic uncertainties.

Acknowledgement: This work was supported in part of the Open Funds from National Key Laboratory of Aerospace Flight Dynamics and Key Laboratory of Space Intelligent Control Technology.

Conflicts of Interest: The authors declare that they have no conflicts of interest to report regarding the present study.

References

Bechlioulis, C. P.; Heshmati-alamdari, S.; Karras, G. C.; Kyriakopoulos, K. J. (2019): Robust image-based visual servoing with prescribed performance under field of view constraints. *IEEE Transactions on Robotics*, vol. 99 (to be published).

Bechlioulis, C. P.; Rovithakis, G. A. (2008): Robust adaptive control of feedback

linearizable mimo nonlinear systems with prescribed performance. *IEEE Transactions on Automatic Control*, vol. 53, no. 9, pp. 2090-2099.

Broschart, S. B.; Scheeres, D. J. (2005): Control of hovering spacecraft near small bodies: application to asteroid 25143 itokawa. *Journal of Guidance, Control, and Dynamics*, vol. 28, no. 2, pp. 343-354.

Ceriotti, M.; Sanchez, J. P. (2016): Control of asteroid retrieval trajectories to libration point orbits. *Acta Astronautica*, vol. 126, pp. 342-353.

Dai, H.; Jing, X.; Wang, Y.; Yue, X.; Yuan, J. (2018): Post-capture vibration suppression of spacecraft via a bio-inspired isolation system. *Mechanical Systems and Signal Processing*, vol. 105, pp. 214-240.

Dragomir, S. (2017): A note on young's inequality. *Revista de la Real Academia de Ciencias Exactas, Físicas y Naturales. Serie A. Matemáticas*, vol. 111, no. 2, pp. 349-354.

Esfandiari, K.; Abdollahi, F.; Talebi, H. A. (2014): Adaptive control of uncertain nonaffine nonlinear systems with input saturation using neural networks. *IEEE Transactions on Neural Networks and Learning Systems*, vol. 26, no. 10, pp. 2311-2322.

Guelman, M. (2015): Closed-loop control of close orbits around asteroids. *Journal of Guidance, Control, and Dynamics*, vol. 38, no. 5, pp. 854-860.

Hua, C.; Chen, J.; Li, Y.; Li, L. (2018): Adaptive prescribed performance control of half-car active suspension system with unknown dead-zone input. *Mechanical Systems and Signal Processing*, vol. 111, pp. 135-148.

Jee, J. R.; Khatib, A. R.; Muellerschoen, R. J.; Williams, B. G.; Vincent, M. A. (1988): Preliminary performance analysis of an interplanetary navigation system using asteroid based beacons. *Journal of Guidance Control and Dynamics*, vol. 11, no. 2, pp. 103-109.

Kumar, K. (2008): Attitude dynamics and control of satellites orbiting rotating asteroids. *Acta Mechanica*, vol. 198, no. 1-2, pp. 99-118.

Lee, D.; Sanyal, A. K.; Butcher, E. A.; Scheeres, D. J. (2015): Finite-time control for spacecraft body-fixed hovering over an asteroid. *IEEE Transactions on Aerospace and Electronic Systems*, vol. 51, no. 1, pp. 506-520.

Lee, K. W.; Singh, S. N. (2019): Adaptive and supertwisting adaptive spacecraft orbit control around asteroids. *Journal of Aerospace Engineering*, vol. 32, no. 4, 04019042.

Li, X.; Luo, X.; Wang, J.; Guan, X. (2018): Finite-time consensus of nonlinear multi-agent system with prescribed performance. *Nonlinear Dynamics*, vol. 91, no. 4, pp. 2397-2409.

Liu, J.; Zhang, Y.; Sun, C.; Yu, Y. (2019): Fixed-time consensus of multi-agent systems with input delay and uncertain disturbances via event-triggered control. *Information Sciences*, vol. 480, pp. 261-272.

Liu, M.; Shao, X.; Ma, G. (2019): Appointed-time fault-tolerant attitude tracking control of spacecraft with double-level guaranteed performance bounds. *Aerospace Science and Technology*.

Liu, Y.; Liu, X.; Jing, Y. (2018): Adaptive neural networks finite-time tracking control for non-strict feedback systems via prescribed performance. *Information Sciences*, vol. 468, pp. 29-46.

Liu, Y.; Lu, S.; Li, D.; Tong, S. (2016): Adaptive controller design-based ablf for a class of nonlinear time-varying state constraint systems. *IEEE Transactions on Systems, Man, and Cybernetics: Systems*, vol. 47, no. 7, pp. 1546-1553.

Luo, J.; Wei, C.; Dai, H.; Yuan, J. (2018): Robust ls-svm-based adaptive constrained control for a class of uncertain nonlinear systems with time-varying predefined performance. *Communications in Nonlinear Science and Numerical Simulation*, vol. 56, pp. 561-587.

Scheeres, D.; Williams, B.; Miller, J. (2000): Evaluation of the dynamic environment of an asteroid: applications to 433 eros. *Journal of Guidance, Control, and Dynamics*, vol. 23, no. 3, pp. 466-475.

Vetrisano, M.; Colombo, C.; Vasile, M. (2016): Asteroid rotation and orbit control via laser ablation. *Advances in Space Research*, vol. 57, no. 8, pp. 1762-1782.

Wei, C.; Luo, J.; Dai, H.; Yin, Z.; Yuan, J. (2017): Low-complexity differentiator-based decentralized fault-tolerant control of uncertain large-scale nonlinear systems with unknown dead zone. *Nonlinear Dynamics*, vol. 89, no. 4, pp. 2573-2592.

Wei, C.; Luo, J.; Dai, H.; Yuan, J.; Xie, J. (2017): Efficient adaptive constrained control with time-varying predefined performance for a hypersonic flight vehicle. *International Journal of Advanced Robotic Systems*, vol. 14, no. 2, 1729881416687504.

Wie, B. (2008): Dynamics and control of gravity tractor spacecraft for asteroid deflection. *Journal of Guidance, Control, and Dynamics*, vol. 31, no. 5, pp. 1413-1423.

Yang, H.; Bai, X.; Baoyin, H. (2016): Finite-time control for asteroid hovering and landing via terminal sliding-mode guidance. *Acta Astronautica*, vol. 132, pp. 78-89.

Yang, H.; Baoyin, H. (2015): Fuel-optimal control for soft landing on an irregular asteroid. *IEEE Transactions on Aerospace and Electronic Systems*, vol. 51, no. 3, pp. 1688-1697.

Yin, Z.; Luo, J.; Wei, C. (2019): Quasi fixed-time fault-tolerant control for nonlinear mechanical systems with enhanced performance. *Applied Mathematics and Computation*, vol. 352, pp. 157-173.

Yin, Z.; Suleman, A.; Luo, J.; Wei, C. (2019): Appointed-time prescribed performance attitude tracking control via double performance functions. *Aerospace Science and Technology*, vol. 93, 105337.

Zeng, X.; Gong, S.; Li, J.; Alfriend, K. T. (2016): Solar sail body-fixed hovering over elongated asteroids. *Journal of Guidance, Control, and Dynamics*, pp. 1223-1231.

Zhang, F.; Duan, G. R. (2014): Robust adaptive integrated translation and rotation finite-time control of a rigid spacecraft with actuator misalignment and unknown mass property. *International Journal of Systems Science*, vol. 45, no. 5, pp. 1007-1034.

Zhao, K.; Song, Y.; Ma, T.; He, L. (2017): Prescribed performance control of uncertain euler-lagrange systems subject to full-state constraints. *IEEE Transactions on Neural Networks and Learning Systems*, vol. 29, no. 8, pp. 3478-3489.